Supporting Information

Helical Nonracemic Tubular Coordination Polymer Gelators from Simple Achiral Molecules

Shiyong Zhang, Shengyong Yang, Jingbo Lan, Shuaijun Yang and Jingsong You*

Key Laboratory of Green Chemistry and Technology of Ministry of Education, College of Chemistry, and State Key Laboratory of Biotherapy, West China Hospital, Sichuan University, Chengdu 610064, People's Republic of China

Tel: 86-28-85412203; *Fax*: 86-28-85412203; E-mail: jsyou@scu.edu.cn

1. General remarks

Unless otherwise noted, all reagents were obtained from commercial suppliers and used without further purification. Dimethyl sulfoxide (DMSO) was dried over CaH_2 for at least 8 h and distilled prior to use. CuI should be washed with THF using a Soxhlet extractor before use to ensure satisfactory catalytic activity.

^1H NMR spectra were obtained with a Varian INOVA-400 (400 MHz), while ^{13}C NMR spectra were recorded on a Varian INOVA-400 (100 MHz) or a Bruker AC-E200 (50 MHz). Mass spectra were obtained by a BioTOF Q or a Finnigan-LCQ^{DECA} instrument. Elemental analyses were performed with a CARLO ERBA1106 instrument.

Absorption spectra were obtained with a UV-Vis TU-1901 spectrophotometer. CD spectra were recorded on a JASCO J-500C spectrophotometer. In the gel phase, the intensity of peaks was too strong to obtain reliable spectra using a conventional optical cell. Therefore, very thin membranes were prepared by sandwiching samples between two quartz glass plates, and subsequently subjected to UV and CD spectral

measurements, so that the ordinate is expressed with an arbitrary unit in Fig. 3. TEM studies were carried out on a JEM-100CXII (Fig. 2a) or a HITACHI H-600 (Fig. S2 and S3), operating at 100 kV. The TEM specimens were prepared by gently placing a copper grid (for Fig. S2 and S3) or a carbon-coated copper grid (for Fig. 2a) on the surface of the sample. The TEM grid was then removed, stained with uranyl acetate or phosphotungstic acid, dried for 0.5 h at room temperature, and then subjected to TEM observation. To obtain the clear TEM images of high resolution, the different straining methods were adopted to provide contrast, and without staining no distinguishable structures were visible due to lack of electron density contrast. A JSM-5900LV scanning electron microscope (SEM) was used for taking the pictures at 20 kV. The preparation of sample for SEM was as follows. The gel in CH_3OH-H_2O was frozen by liquid nitrogen, and the frozen specimen was then evaporated by a vacuum pump at -38 °C for 1 day. The obtained xerogel was shielded with gold and then examined. Tapping mode AFM imaging was performed under ambient conditions on a SEIKO SPA400 instrument by using BS-Tap 300Al levers (Budget Sensors, silicone cantilevers). Samples of $\{[Ag\text{-}\mathbf{2}]NO_3\}_n$ (0.08 wt%) in CH_3OH-H_2O (3:2 wt/wt) were cast onto a freshly cleaved mica under ambient conditions, and then left open to the atmosphere for half a day before making AFM images.

2. General synthetic procedure for ligands 1-5[1]

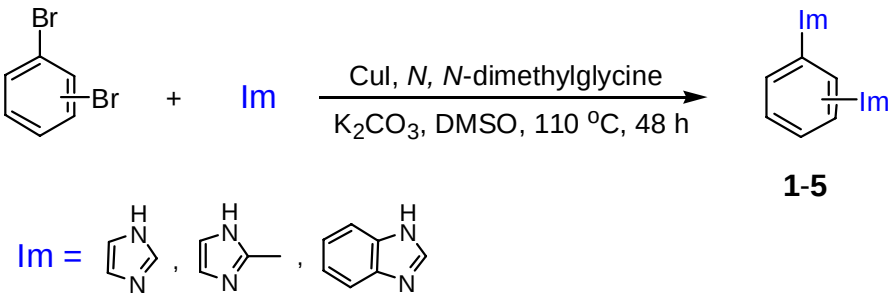

Scheme S1 Synthesis of rigid ligands **1-5**.

A Schlenk flask was charged with CuI (4 mmol), *N*, *N*-dimethylglycine (8 mmol), K_2CO_3 (80 mmol), aryl bromide (20 mmol), and the imidazole derivative (50 mmol).

The system was then evacuated twice and back filled with N_2, followed by addition of 50 mL of DMSO. The mixture was heated at 110 °C for 48 h before it was partitioned between water and ethyl acetate. The organic layer was separated, and the aqueous layer was extracted with ethyl acetate. The combined organic layers were washed with brine, dried over $MgSO_4$, and concentrated in vacuo. The residue was loaded on a silica gel column and eluted with CH_2Cl_2/CH_3OH (10/1) to give a pale yellow solid, which could be recrystallized from CH_3OH to afford the pure bisimidazole.

1,2-Bis(1-imidazolyl)benzene (1): white crystals. Yield: 21 %. Mp: 136-137 °C. ^{1}H NMR (400 MHz, $CDCl_3$): δ 7.59-7.55 (m, 2H), 7.52-7.49 (m, 2H), 7.46 (s, 2H), 7.11 (s, 2H), 6.75 (s, 2H). ^{13}C NMR (100 MHz, $CDCl_3$): δ 136.6, 132.1, 130.5, 129.5, 127.0, 119.3. ESI-MS (*m/z*): 211.2 $[M + H]^+$. Anal. Calcd for $C_{12}H_{10}N_4$: C 68.56, H 4.79, N 26.65. Found: C 68.40, H 4.88, N 26.72.

1,3-Bis(1-imidazolyl)benzene (2): white crystals. Yield: 93 %. Mp: 145-146 °C (lit[2] 136-137 °C). ^{1}H NMR (400 MHz, $CDCl_3$): δ 7.90 (s, 2H), 7.60 (t, *J* = 8.0 Hz, 1H), 7.43-7.41 (m, 2H), 7.39 (d, *J* = 1.6 Hz, 1H), 7.32 (s, 2H), 7.23 (s, 2H). ^{13}C NMR (50 MHz, $CDCl_3$): δ 136.7, 135.5, 131.5, 131.0, 120.2, 116.1, 114.6. ESI-MS (*m/z*): 211.0 $[M + H]^+$. Anal. Calcd for $C_{12}H_{10}N_4$: C 68.56, H 4.79, N 26.65. Found: C 68.64, H 4.85, N 26.55.

1,3-Bis(2-methyl-1-imidazolyl)benzene (3): white crystals. Yield: 88 %. Mp: 176-177 °C. ^{1}H NMR (400 MHz, $CDCl_3$): δ 7.60 (t, *J* = 8.0 Hz, 1H), 7.37 (d, *J* = 2.4 Hz, 1H), 7.35 (d, *J* = 2.0 Hz, 1H), 7.25 (t, *J* = 2.0 Hz, 1H), 7.04 (d, *J* = 2.4 Hz, 4H), 2.40 (s, 6H). ^{13}C NMR (50 MHz, $CDCl_3$): δ 144.4, 136.7, 130.4, 126.1, 124.8, 122.2, 120.3, 13.7. ESI-MS (*m/z*): 239.1 $[M + H]^+$. Anal. Calcd for $C_{14}H_{14}N_4$: C 70.57, H 5.96, N 23.51. Found: C 70.67, H 5.92, N 23.29.

1,4-Bis(1-imidazolyl)benzene (4): white crystals. Yield: 95 %. Mp: 216-217 °C (lit[3] 216-217 °C). ^{1}H NMR (400 MHz, $CDCl_3$): δ 7.89 (t, *J* = 1.2 Hz, 2H), 7.54 (s, 4H), 7.32 (t, *J* = 1.6 Hz, 2H), 7.25 (t, *J* = 1.2 Hz, 2H). ^{13}C NMR (100 MHz, $CDCl_3$): δ 136.4, 135.5, 130.9, 122.8, 118.1. ESI-MS (*m/z*): 211.3 $[M + H]^+$. Anal. Calcd for $C_{12}H_{10}N_4$: C 68.56, H 4.79, N 26.65. Found: C 68.56, H 4.80, N 26.60.

1,3-Bis(1-benzo[d]imidazolyl)benzene (5): pale yellow crystals. Yield: 90 %. Mp:

204-205 °C. ^{1}H NMR (400 MHz, $CDCl_3$): δ 8.20 (s, 2H), 7.92-7.90 (m, 2H), 7.84 (t, *J* = 8.0 Hz, 1H), 7.74 (s, 1 H), 7.66 (d, *J* = 8 Hz, 2H), 7.62-7.60 (m, 2H), 7.40-7.37 (m, 4H). ^{13}C NMR (100 MHz, $CDCl_3$): δ 144.1, 141.9, 138.1, 133.3, 131.8, 124.2, 123.3, 123.1, 120.9, 119.2, 110.1. ESI-MS (*m/z*): 311.4 $[M + H]^+$. Anal. Calcd for $C_{20}H_{14}N_4$: C 77.40, H 4.55, N 18.05. Found: C 77.42, H 4.43, N 17.82.

3. Gelation Test

A methanol (4 mL) solution of **2** (0.05 mmol) was added into an aqueous (2 mL) solution of $AgNO_3$ (0.05 mmol) in a septum-capped test tube under continuous shaking at room temperature in the absence of light. After the mixture was placed for about 5 min, the transparent gel, which was evaluated by the "stable to inversion of a test tube" method, was formed. The gel obtained from this method usually has some air bubbles, which could be removed by sonication. The results of gelation test in a wide range of solvents have been shown in Table S1.

A stronger gel could be obtained by slow diffusion between two layers of a methanol solution of **2** and an aqueous solution of $AgNO_3$ at room temperature for about 2 weeks. The gel afforded could be stably maintained over a period of half-year at ambient temperature.

Sol-gel phase transfer temperature (T_{gel}) was determined by placing an inverted, sealed tube in a thermocontrolled oil bath while increasing the temperature at a rate of 1 °C per minute. Here, T_{gel} is defined as the temperature at which the solvent begins to flow out of the gel.

4. Optimization of the ratio of organic solvent and water in gelation test

T_{gel} were measured at different ratios of H_2O/CH_3OH on the basis of 1.0 wt% of the $\{[Ag\text{-}\mathbf{2}]NO_3\}_n$ as gelator. Fig. S1 shows a clear maximum at the 3/2 ratio of CH_3OH/H_2O, which was considered as the optimal ratio.

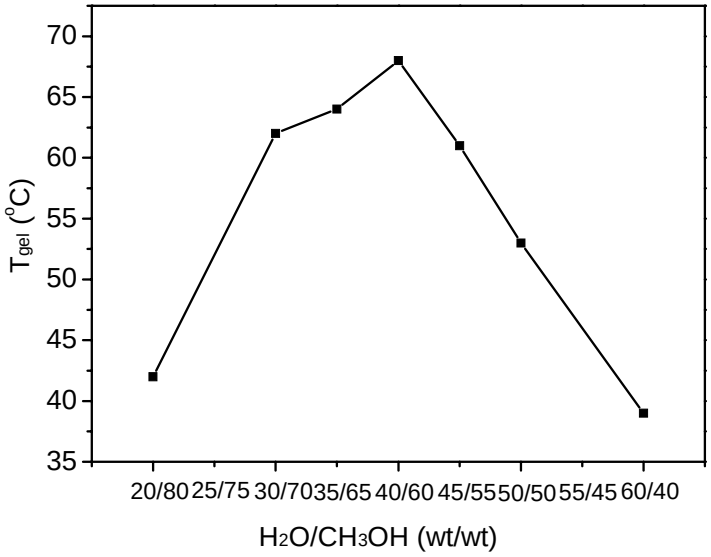

Fig. S1 Plot of T_{gel} vs. H_2O/CH_3OH (wt/wt). The $\{[Ag\text{-}\mathbf{2}]NO_3\}_n$ gelator is 1.0 wt%.

5. Gelation test of the $\{[Ag\text{-}2]NO_3\}_n$ in different solvents

Table S1 Gelation test of the $\{[Ag\text{-}\mathbf{2}]NO_3\}_n$ in different solvents[a]

Entry	Solvent[b]	Result
1	dimethyl sulfoxide (DMSO)	S
2	Dimethylformamide (DMF)	G[c]
3	CH_3OH-H_2O	G[d]
4	CH_3CH_2OH-H_2O	G
5	*i*-propanol-H_2O	G
6	*t*-butanol-H_2O	G
7	$PhCH_2OH$-H_2O	Gp
8	CH_2=$CHCH_2OH$-H_2O	G
9	*n*-$CH_3CH_2CH_2CH_2OH$	Gp
10	$HOCH_2CH_2OH$	G
11	CH_3CN-H_2O	G
12	CH_3NO_2	S
13	CH_2Cl_2-H_2O	G
14	$CHCl_3$-H_2O	G
15	$ClCH_2CH_2Cl$-H_2O	P
16	CCl_4	P
17	$CH_3COOCH_2CH_3$-H_2O	P
18	CH_3COOH -H_2O	G

[a] Gelator: 2.0 wt%. S: solution; G: steady gel; Gp: partial gel; P: precipitate. [b] In the case of mixed solvents, the ratio of organic solvent and water is 3:2 (wt/wt). [c] Gelator: 0.4 wt%. [d] Gelator: 0.3 wt%.

6. Morphology analysis of the {[Ag-2]NO_3}$_n$ aggregates

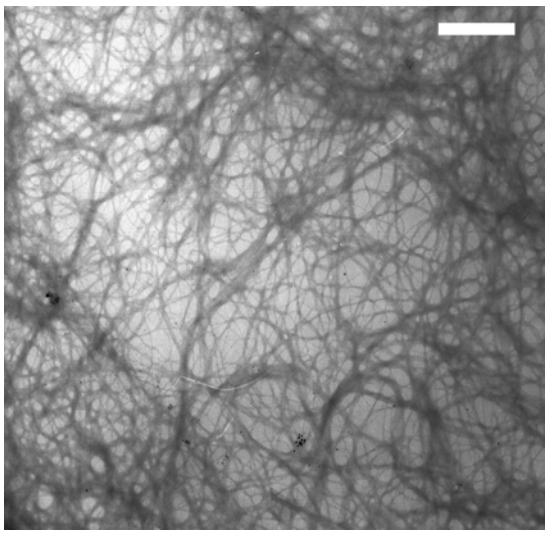

Fig. S2 TEM image of the {[Ag-**2**]NO_3}$_n$ gel (0.8 wt%) in CH_3OH-H_2O (3:2 wt/wt), unstained. The scale bar corresponds to 1 μm.

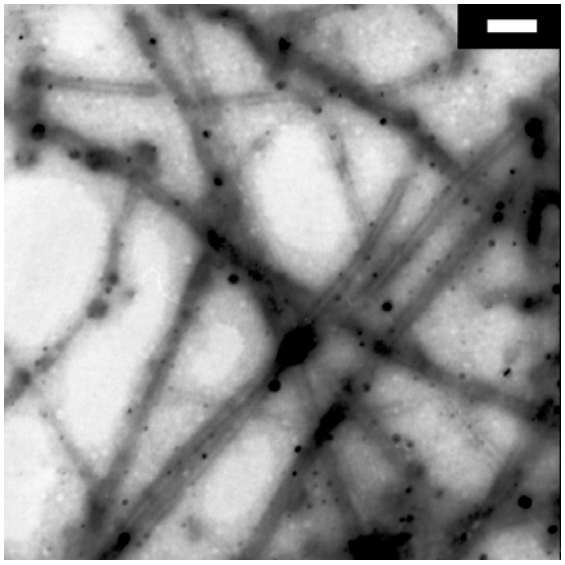

Fig. S3 TEM image of the aggregates of {[Ag-**2**]NO_3}$_n$ (0.1 wt%) in CH_3OH-H_2O (3:2 wt/wt), stained with phosphotungstic acid aqueous solution (10 g dm^{-3}). The black dots are the phosphotungstic acid aggregates. The scale bar corresponds to 100 nm.

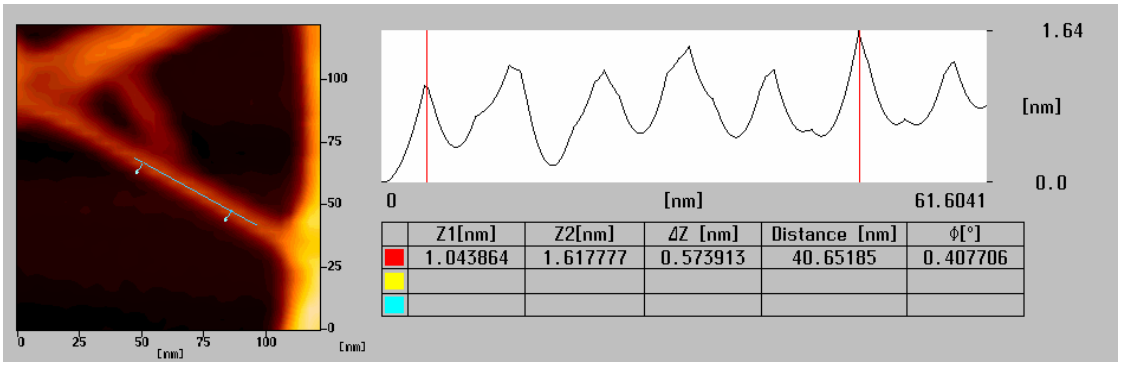

Fig. S4 Line-scan profile along a single tubule revealing an average helical pitch of ca. 8.0 nm.

7. Theoretical calculation

In order to understand the formation mechanism of helical tubular polymers, theoretical calculations based on the first principle density functional theory (DFT) have been carried out to model the assembly of 1,3-bis(1-imidazolyl)benzene and silver ion. As has been known, the coordination number of silver is two, and obviously the 1,3-bis(1-imidazolyl)benzene has two coordination sites (the terminal imine nitrogen), with each one coordinating to different silver ion. The remaining coordination site of the silver can also be coordinated by an imine in another 1,3-bis(1-imidazolyl)benzene (Fig. S5). Consequently the 1,3-bis(1-imidazolyl)-benzene and silver ion occur alternatively, finally forming the polymer. Apparently, geometry of 1,3-bis(1-imidazolyl)benzene and the coordination mode between 1,3-bis(1-imidazolyl)benzene and silver ion are key factors to determine the final topological structure of the polymer formed. Therefore, we shall firstly calculate the structure of 1,3-bis(1-imidazolyl)benzene, then construct a short polymer (for an example, trimer) based on the most stable 1,3-bis(1-imidazolyl)benzene followed by performing geometry optimization to the constructed polymer, which purpose is to obtain some geometry parameters that can be used to build more longer polymer.

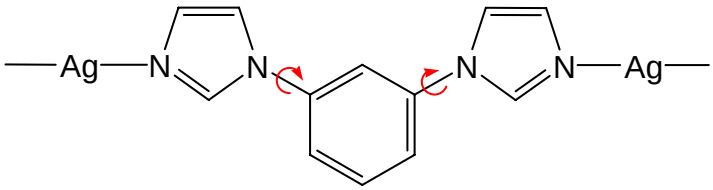

Fig. S5 Proposed coordination mode of 1,3-bis(1-imidazolyl)benzene and Ag (I).

Different conformations for 1,3-bis(1-imidazolyl)benzene are possible mainly due to the variations of the dihedral angles between benzene and imidazole rings (as the relative rigidity of the benzene and imidazole rings). A conformation search for 1,3-bis(1-imidazolyl)benzene demonstrated that the energetically most favorable structures correspond to conformations with dihedral angle of ca. 45.5º between the imidazole and benzene planes (Fig. S6A). The coplanar structure (Fig. S6B) is not favored due to the repulsive interaction of conjugated π-electrons between the imidazole and benzene rings. Actually seven isomers with almost the same dihedral angle but different orientations between imidazole and benzene planes have been located (Fig. S7, **A01**-**A07**). Almost no energy difference for these isomers has been found. However, a real entity model construction demonstrated that conformation **A01**, which presents an open-armed shape, is the only one that has a correct conformation for building a helical tubule.

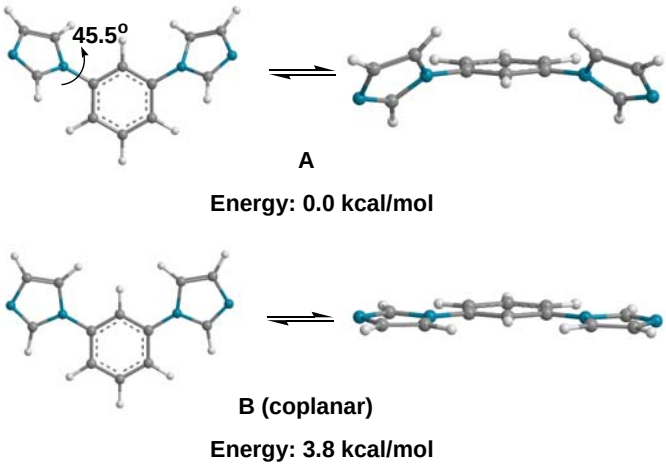

Fig. S6 Optimized structures of 1,3-bis(1-imidazolyl)benzene. **A**, Conformation with dihedral angle of 45.5º between the imidazole and benzene planes. **B**, Coplanar structure between the two planes.

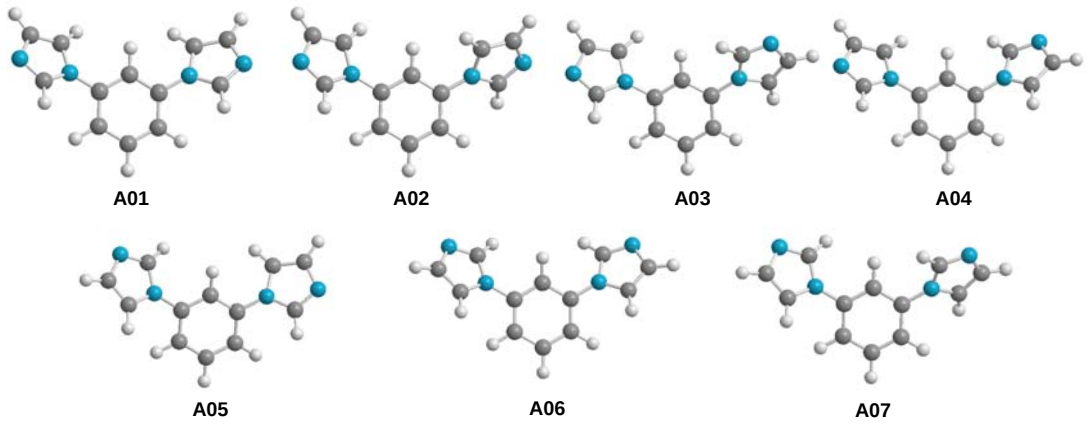

Fig. S7 Possible isomers for the most stable conformation of 1,3-bis(1-imidazolyl)benzene.

Now we explore the coordination mode between 1,3-bis(1-imidazolyl)benzene and silver ion. In order to mimic the real coordination environment of 1,3-bis(1-imidazolyl)benzene and silver ion, a model segment composed of three 1,3-bis(1-imidazolyl)benzene and four silver ions (shorted as **3L4Ag**, Fig. S8) was constructed. The initial structure for the model **3L4Ag** was generated in which the 1,3-bis(1-imidazolyl)benzene adopts conformation **A01**. Full geometry optimization without any constraint for the initial structure of **3L4Ag** was conducted. Fig. S9 shows the optimized structure, which has been confirmed by frequency analysis.

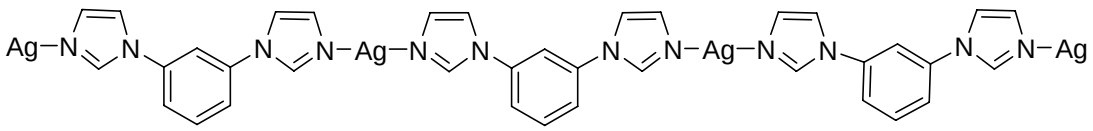

Fig. S8 Constructed model (three 1,3-bis(1-imidazolyl)benzene and four silver ions, denoted as **3L4Ag**).

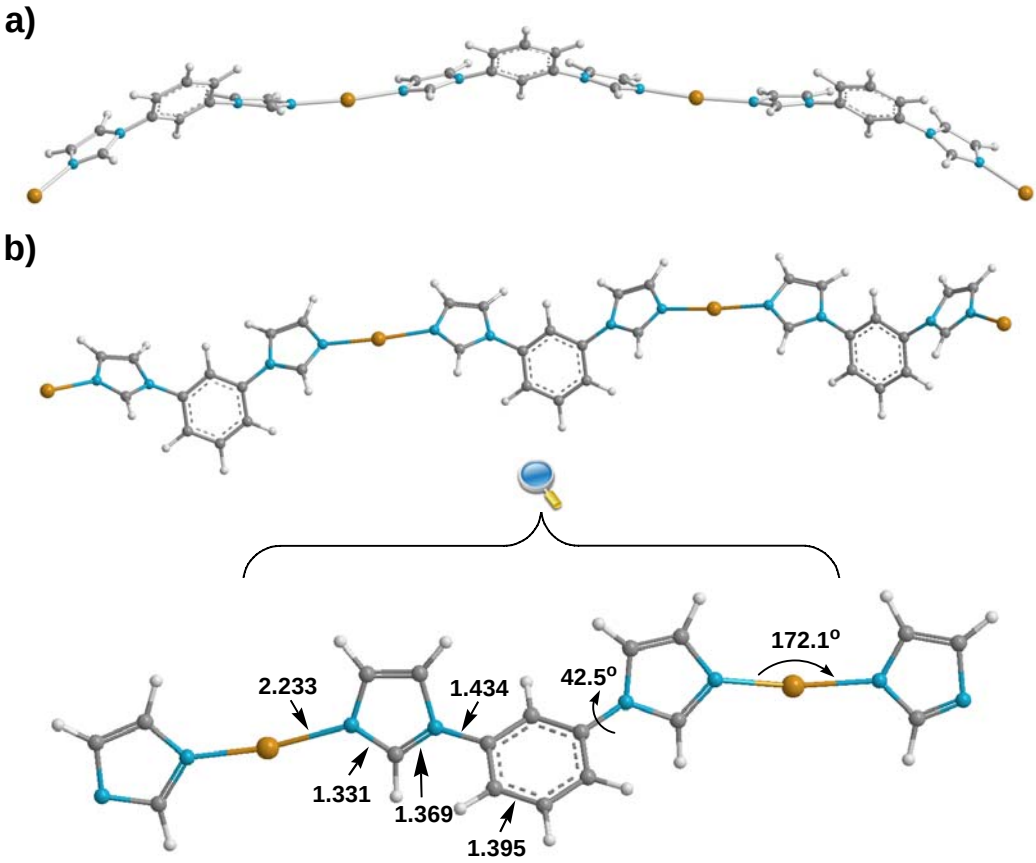

Fig. S9 Optimized structure for the model **3L4Ag** with views from top (a) and front (b). Selected geometry parameters are shown below (bond distances are in Å, angles in degree). Gold, Ag; cyan, N; gray, C; white, H.

From Fig. S9, one can find that the N(imidazolyl)-Ag-N(imidazolyl) is not linear (an angle of ca. 172.1º) due to the strong *trans* influence of the imine (imidazolyl). The dihedral angle between the imidazole and benzene rings is ca. 42.5º, which is a little smaller than that in the pure 1,3-bis(1-imidazolyl)benzene (45.5º). A reasonable explanation is that the silver cations reduce the conjugated π-electrons repulsive interaction between the imidazole and benzene rings in a way. Some small differences in geometry have been found between the terminal and middle 1,3-bis(1-imidazolyl)benzene motif. Since the environment of 1,3-bis(1-imidazolyl)benzene and silver ions locating in the middle of **3L4Ag** is more close to the real case in the complete polymer product, the geometry parameters for the middle 1,3-bis(1-imidazolyl)benzene will make more sense for the whole polymer building.

Finally the 1,3-bis(1-imidazolyl)benzene and one silver ion locating in the middle of **3L4Ag** was taken as a repeating unit. By duplicating the optimized repeating unit, a helical tubular polymer product was obtained (Fig. S10),[4] in which a cycle is approximately composed of 20 1,3-bis(1-imidazolyl)benzene and 21 silver ions. The diameter of the helical tubule is ca. 9.1 nm and the helical pitch length is ca. 7.1 nm, which is almost consistent with the experimental results.

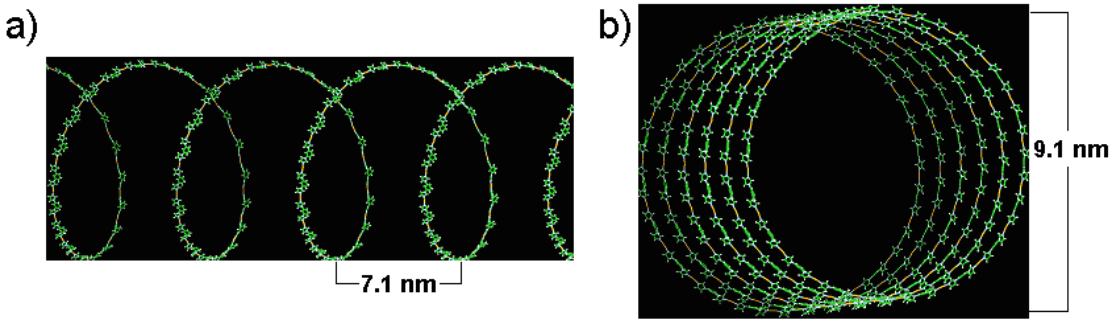

Fig. S10 Helical tubular polymer built by duplicating the optimized repeating unit. a) side view. b) top view.

Computational Details

Theoretical calculations were carried out with the Amsterdam Density Functional (ADF 2005) program package developed by Baerends[5-7] and by Ravenek.[8] The electronic configurations of the atoms were described by a triple-ζ basis set on Silver (4s, 4p, 4d and 5s) and augmented with a single 5p polarization function. Double-ζ STO basis sets were used for carbon (2s, 2p), hydrogen (1s), and nitrogen (2s, 2p), augmented with a single 3d polarization function, except for hydrogen, where a 2p polarization function was used. The $1s^2$, $2s^2$, $2p^6$, $3s^2$, $3p^6$, $3d^{10}$ on Ag, $1s^2$ for C and N were treated with the frozen-core approximation. A set of auxiliary s, p, d, f and g STO functions centered on all nuclei was used to fit the molecular density and represent Coulomb and exchange potentials accurately in each SCF cycle.[9] The energy differences were calculated by augmenting the local density approximation energy with Perdew and Wang's non-local correlation correction and Becke's exchange corrections (PWB91).[10-13]

8. Reference

(1) H. Zhang, Q. Cai and D. Ma, *J. Org. Chem.* **2005**, *70*, 5164.

(2) E. Alcalde, I. Dinarès, S. Rodríguez and C. G. de Miguel, *Eur. J. Org. Chem.* **2005**, 1637.

(3) H.-J. Cristau, P. P. Cellier, J.-F. Spindler and M. Taillefer, *Chem. Eur. J.* **2004**, *10*, 5607.

(4) It should be noted that utilizing the optimized model, both the left and right-handed helical tubule could be obtained, which lies on the initial duplicating direction chosen.

(5) E. J. Baerends, D. E. Ellis and P. Ros, *Chem. Phys.* **1973**, *2*, 41.

(6) E. J. Baerends and P. Ros, *Chem. Phys.* **1973**, *2*, 52.

(7) G. te Velde and E. J. Baerends, *J. Comput. Phys.* **1992**, *99*, 84.

(8) H. J. J. te Riele, T. J. Dekker and H. A. van der Vorst, *Algorithms and application on vector and parallel computers*, Elsevier, Amsterdam, 1987.

(9) J. Krijn and E. J. Baerends, *Fit functions in the HFS-Method*, Free University of Amsterdam, Amsterdam, 1984.

(10) J. P. Perdew, *Phys. Rev. B* **1992**, *46*, 6671.

(11) A. Becke, *Phys. Rev. A* **1988**, *38*, 3098.

(12) J. P. Perdew, *Phys. Rev. B* **1986**, *34*, 7406.

(13) J. P. Perdew, *Phys. Rev. B* **1986**, *33*, 8822.

9. Copies of ^{1}H-NMR and ^{13}C-NMR spectra for 1-5

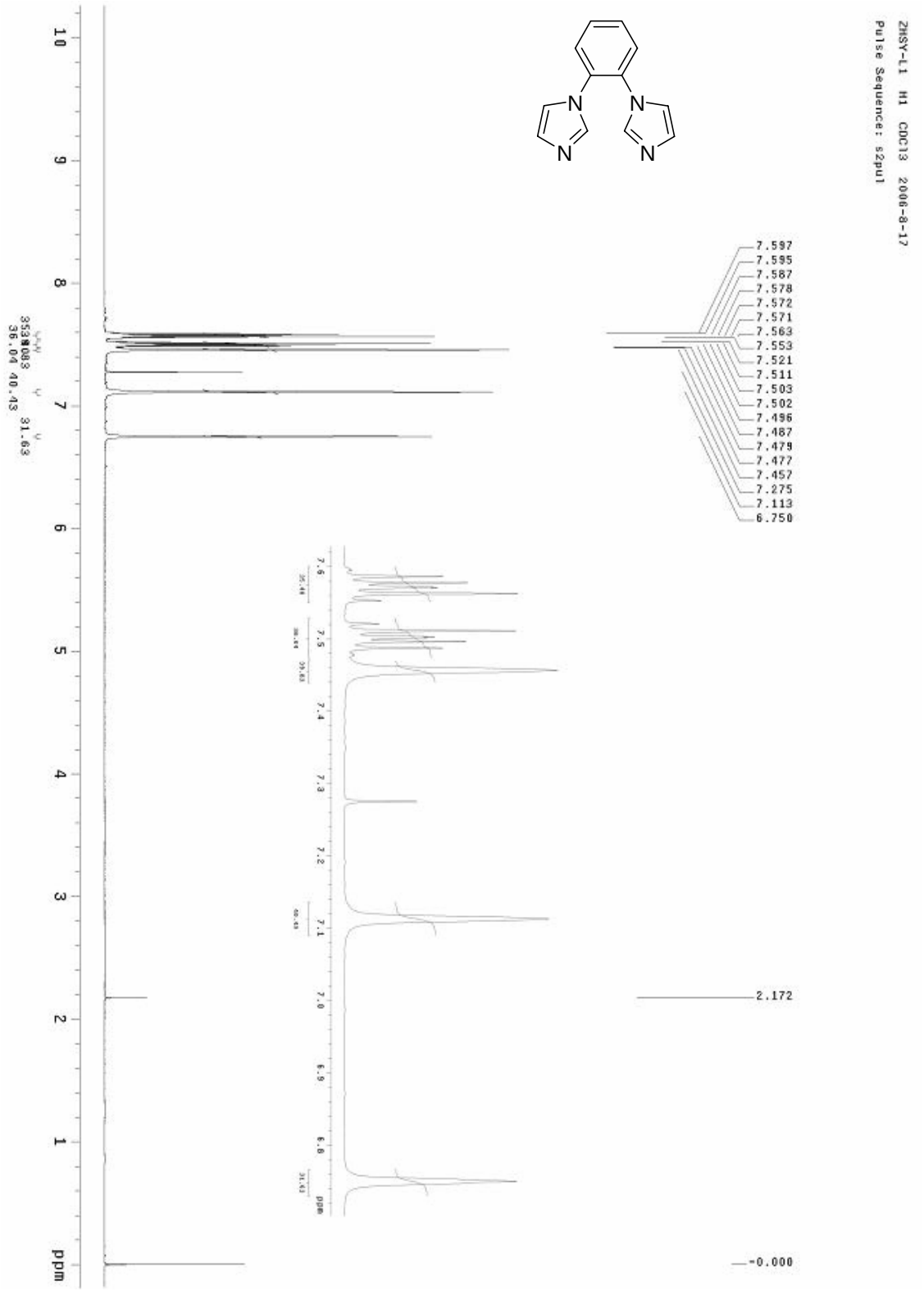

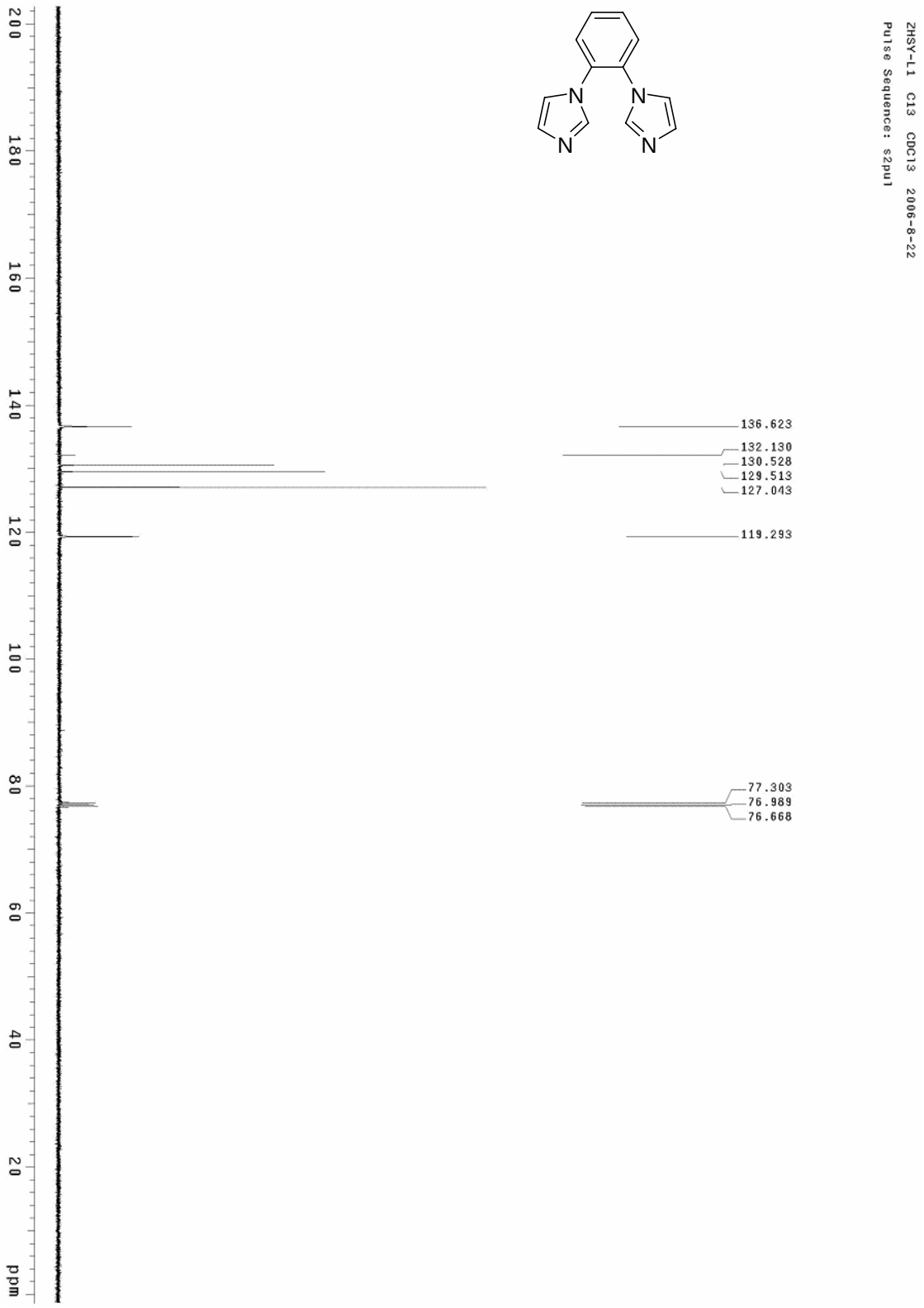
ZHSY-L1 C13 CDCl3 2006-8-22
Pulse Sequence: s2pul
136.623
132.130
130.528
129.513
127.043
119.293
77.303
76.989
76.668
200
180
160
140
120
100
80
60
40
20
ppm

Zhsy-L2-CDCL3-H1-2006-7-18

Pulse Sequence: s2pul

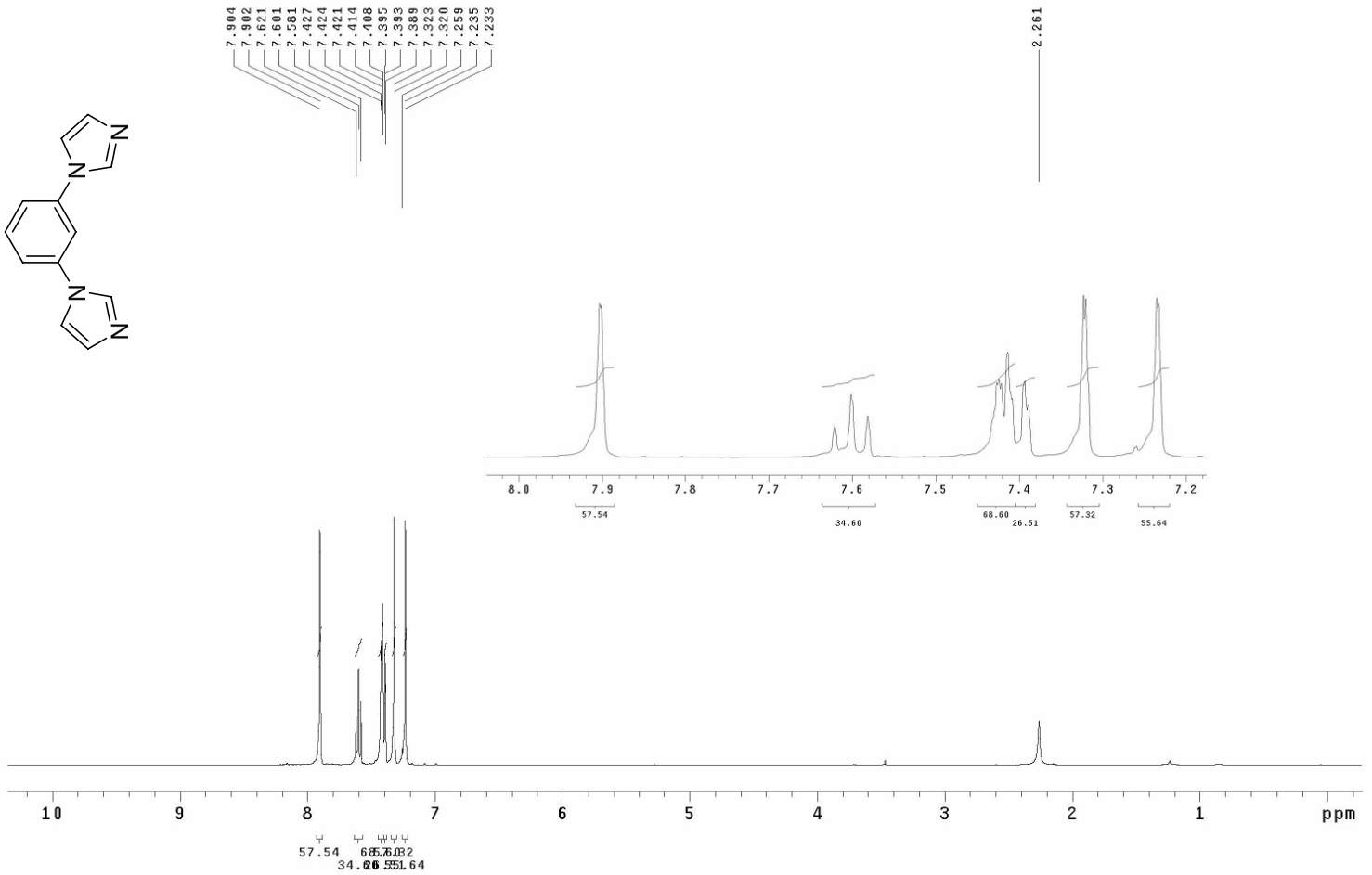

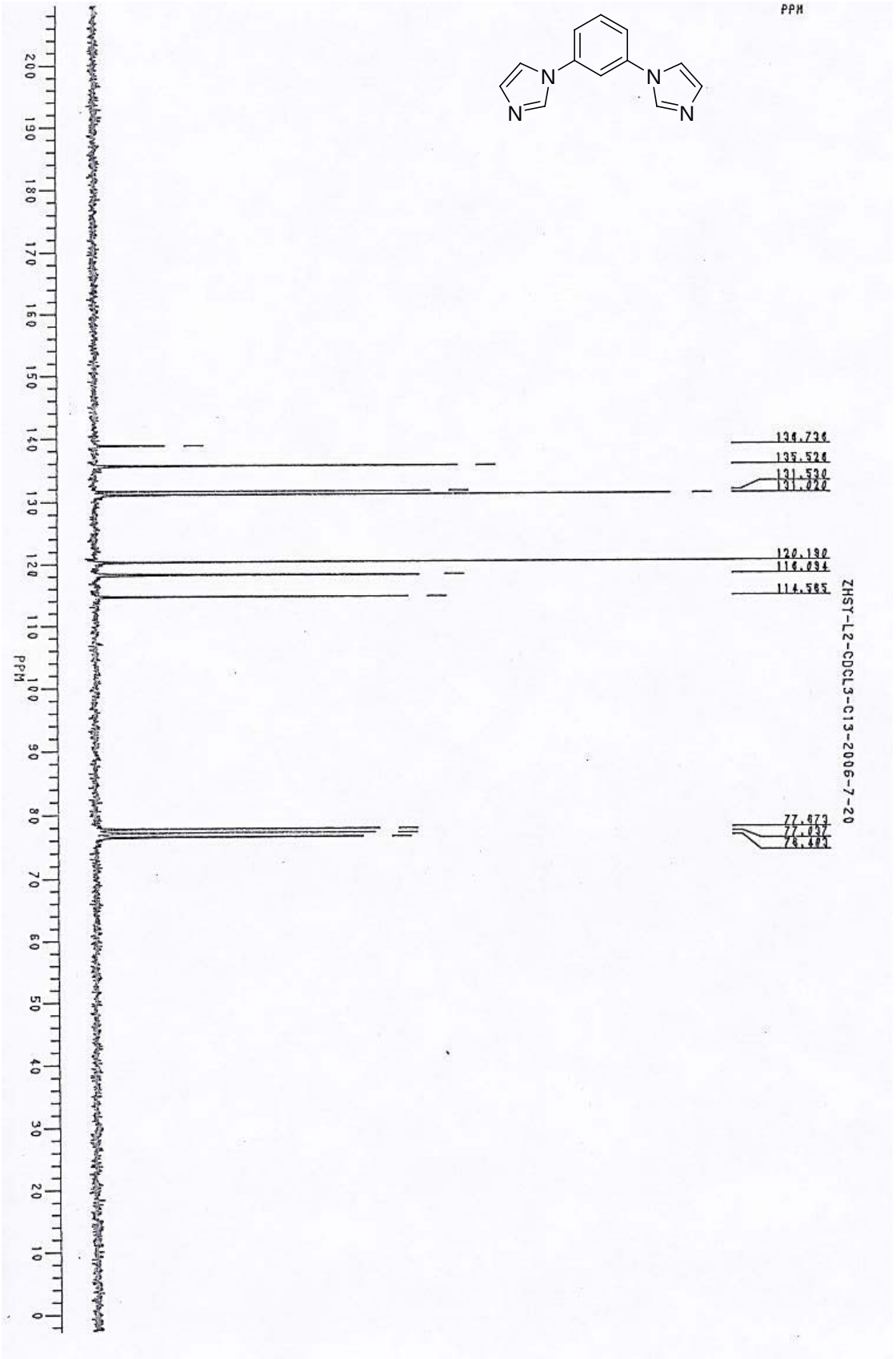
PPM
N
N
N
N
136.736
135.526
131.530
131.020
120.190
116.094
114.585
77.673
77.057
76.443
ZHSY-L2-CDCL3-C13-2006-7-20
PPM
200
190
180
170
160
150
140
130
120
110
100
90
80
70
60
50
40
30
20
10
0

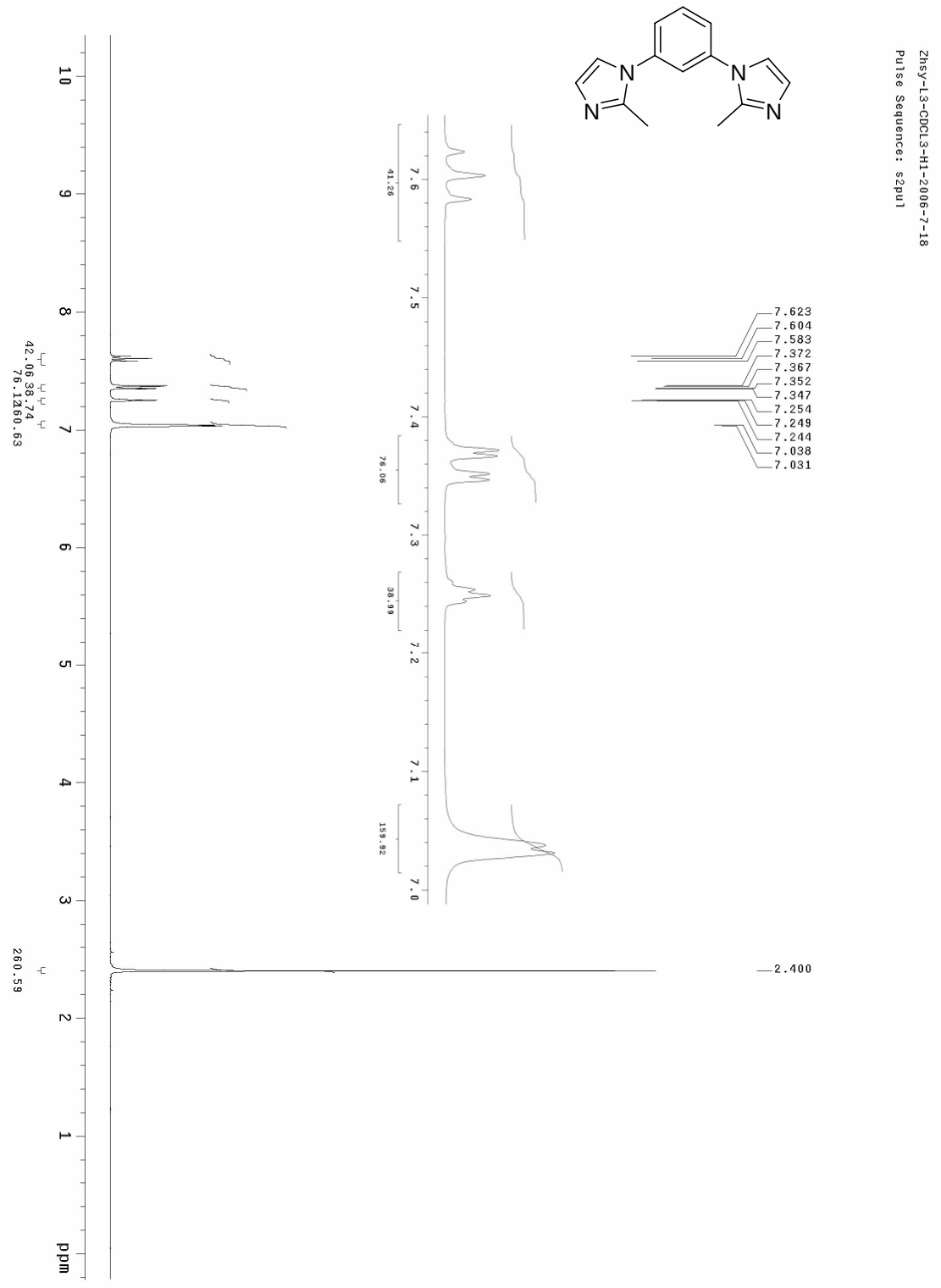
Zhsy-L3-CDCL3-H1-2006-7-18
Pulse Sequence: s2pul
7.623
7.604
7.583
7.372
7.367
7.352
7.347
7.254
7.249
7.244
7.038
7.031
2.400
41.26
76.06
30.99
159.92
42.06
38.74
76.12
60.63
260.59
ppm

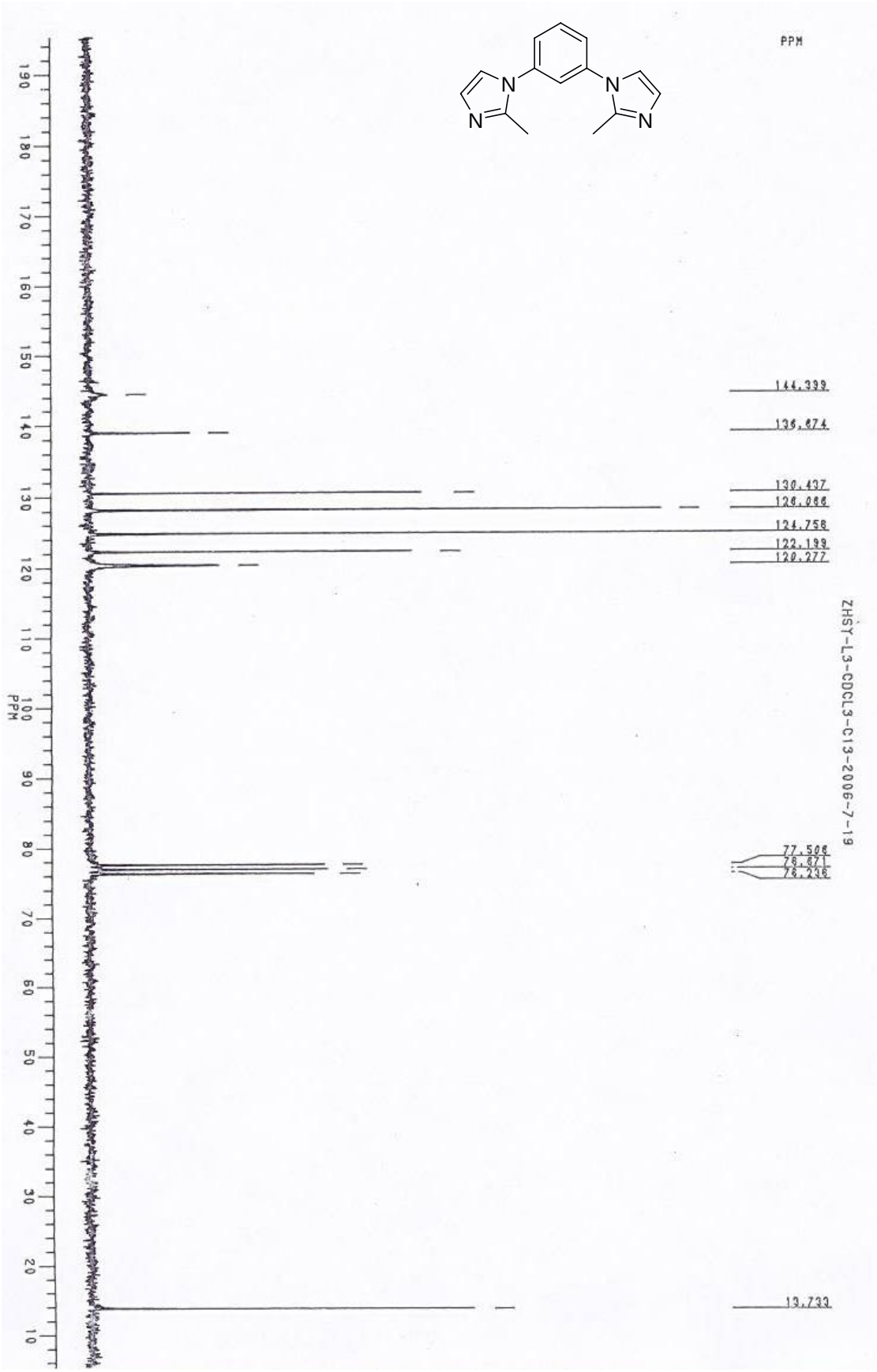
PPM
144.399
136.874
130.437
126.066
124.758
122.199
120.277
77.506
76.871
76.236
13.733
ZHSY-L3-CDCL3-C13-2006-7-19
PPM

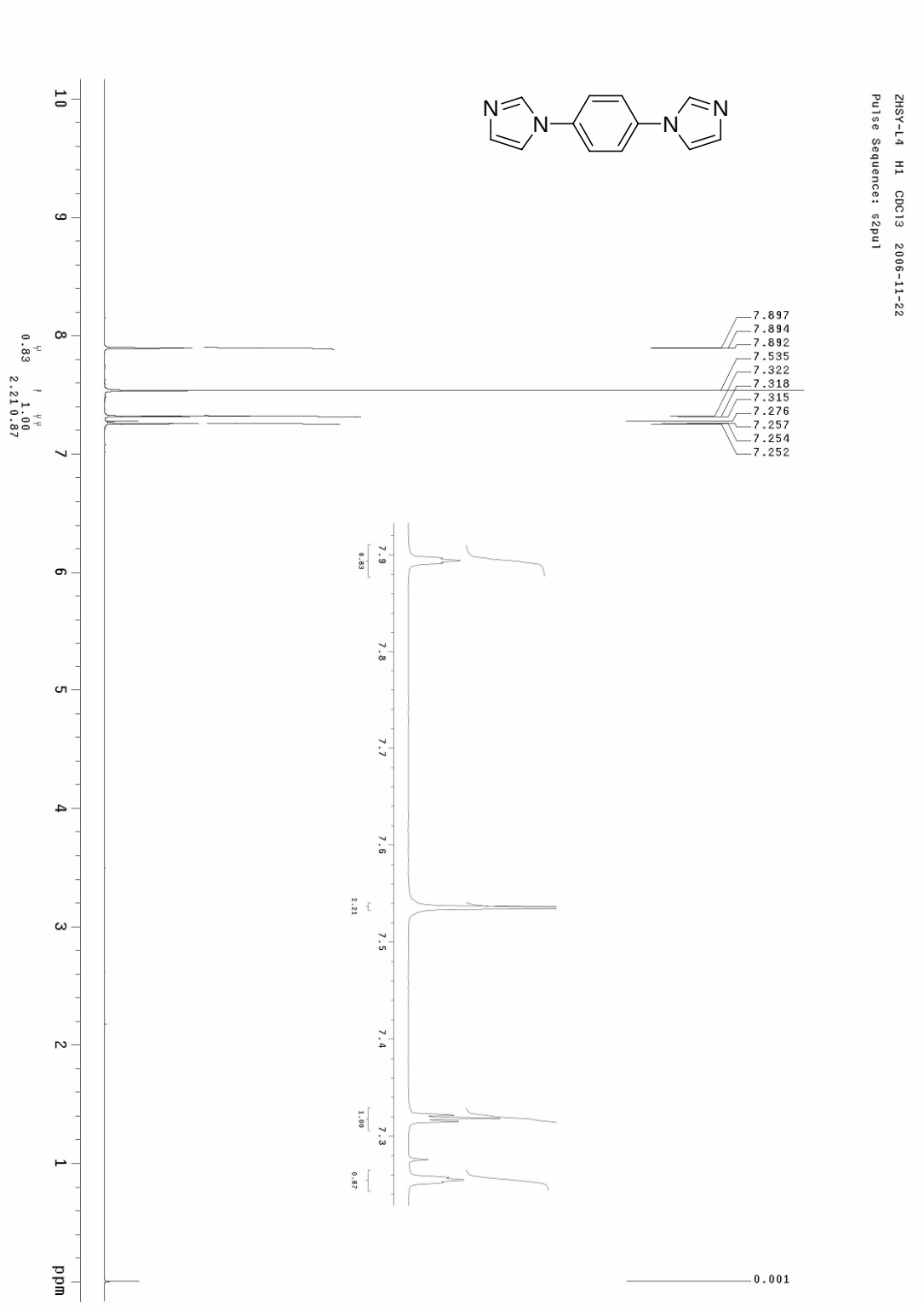
ZHSY-L4 H1 CDCl3 2006-11-22
Pulse Sequence: s2pul
7.897
7.894
7.892
7.535
7.322
7.318
7.315
7.276
7.257
7.254
7.252
0.001
0.83
1.00
2.21
0.87
ppm

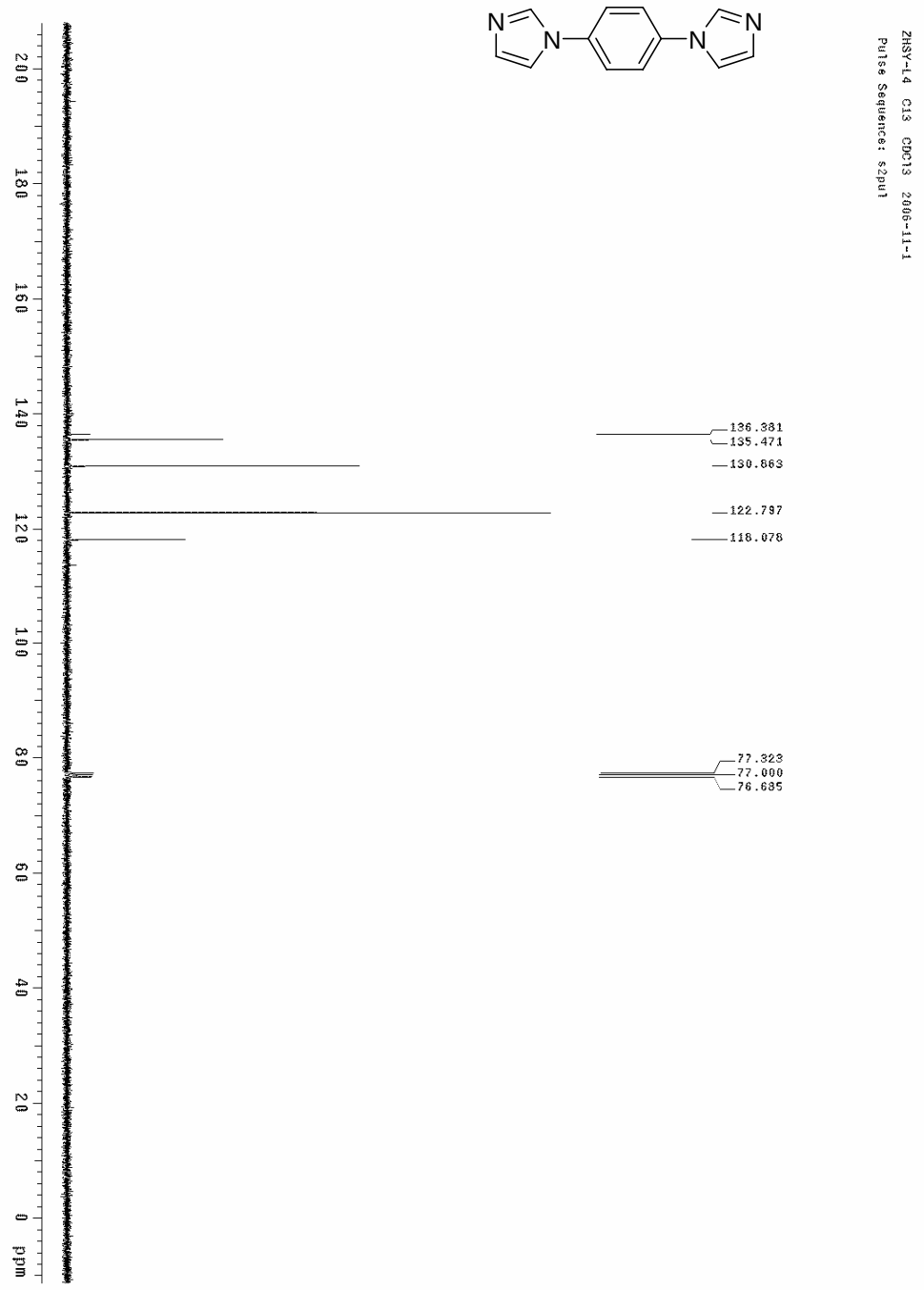
ZHSY-L4 C13 CDCl3 2006-11-1
Pulse Sequence: s2pul
136.381
135.471
130.863
122.797
118.078
77.323
77.000
76.685
200
180
160
140
120
100
80
60
40
20
0
ppm

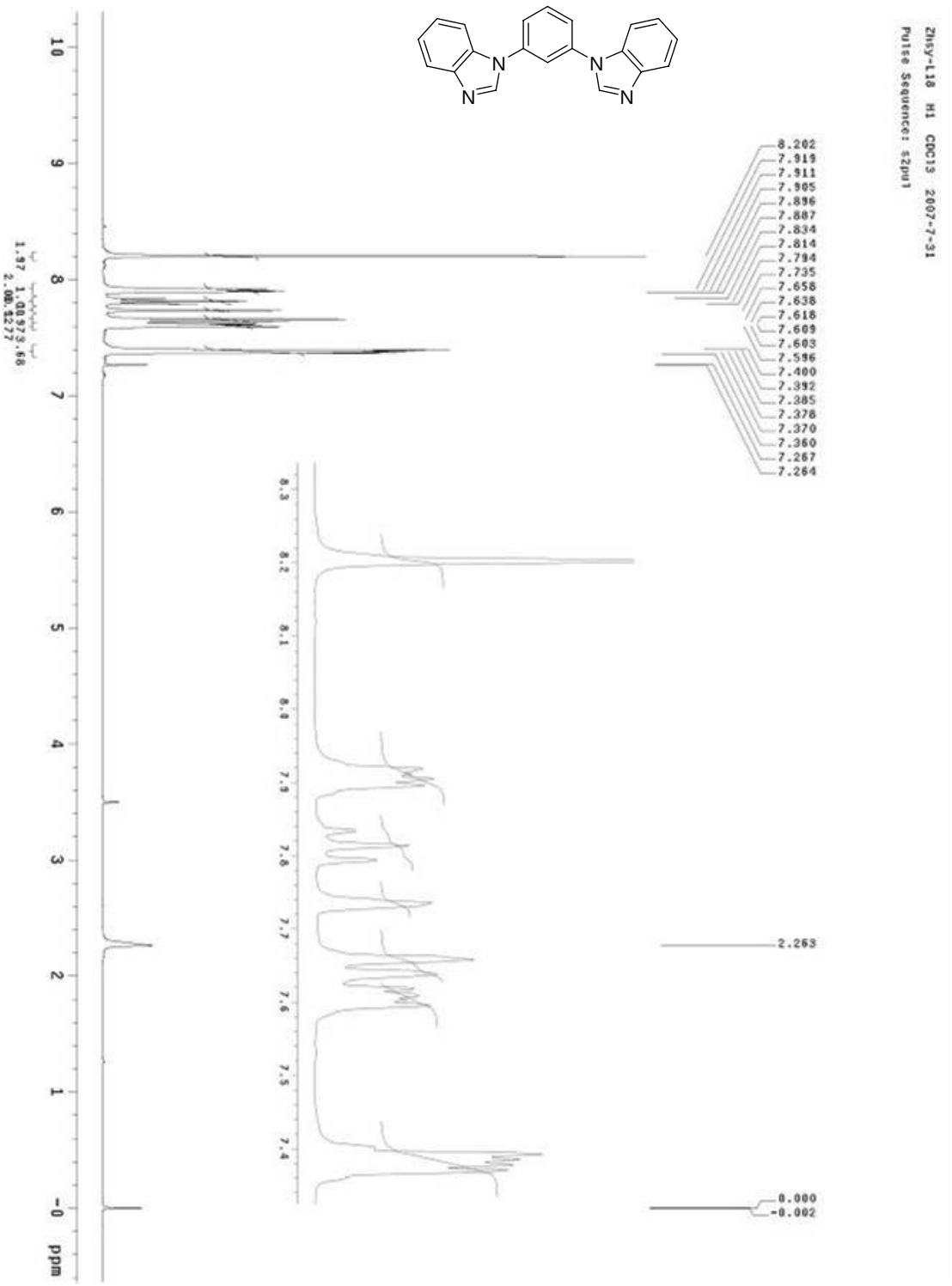
ZhSy-L18 H1 CDCl3 2007-7-31
Pulse Sequence: s2pul
8.202
7.919
7.911
7.905
7.896
7.887
7.834
7.814
7.794
7.735
7.658
7.638
7.618
7.609
7.603
7.596
7.400
7.392
7.385
7.378
7.370
7.360
7.267
7.264
2.263
0.000
-0.002
ppm

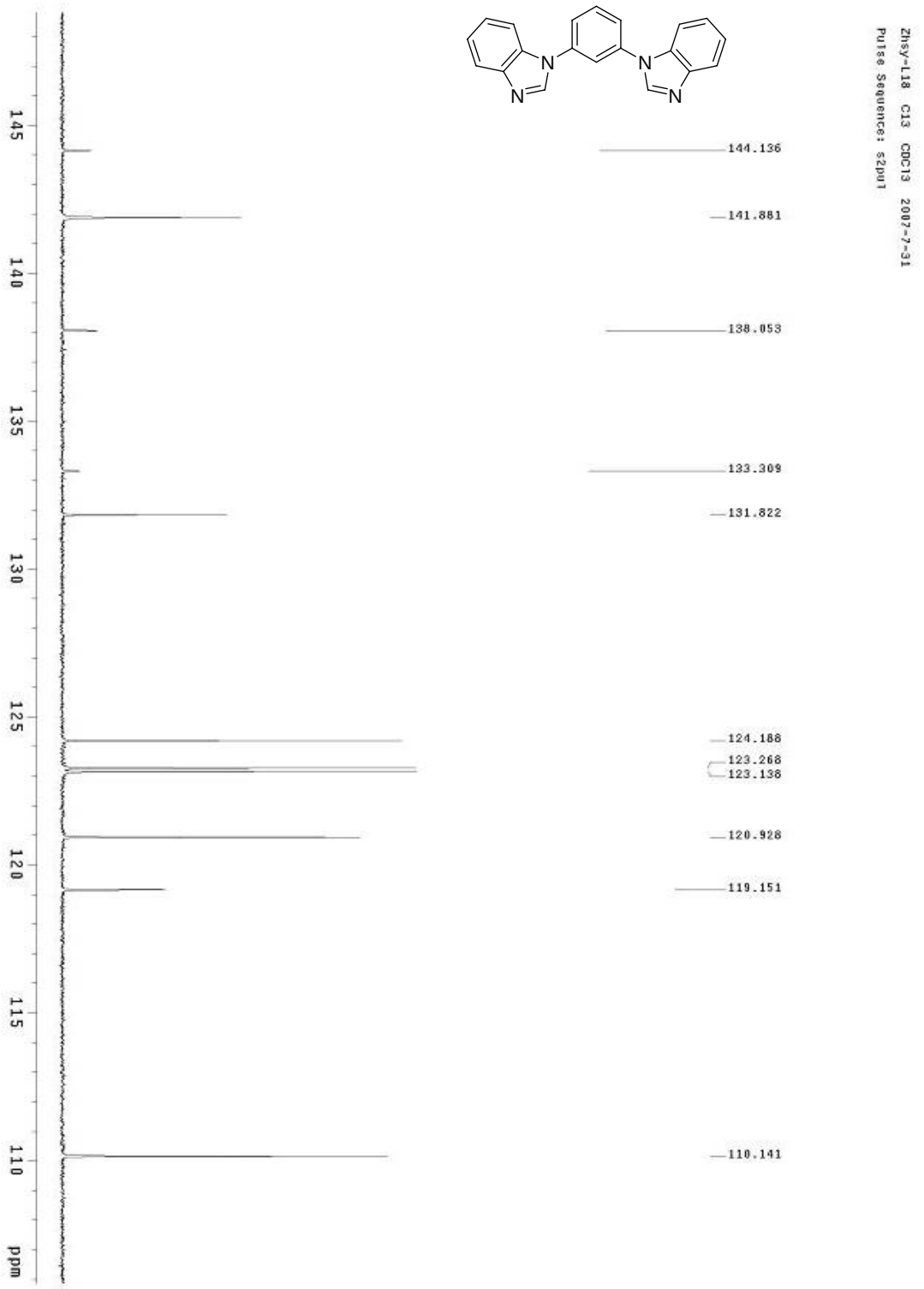
Zhsy-L18 C13 CDCl3 2007-7-31
Pulse Sequence: s2pul
144.136
141.881
138.053
133.309
131.822
124.188
123.268
123.138
120.928
119.151
110.141
145
140
135
130
125
120
115
110
ppm